

Article

High Stability of Liquid-Typed White Light-Emitting Diode with Zn_{0.8}Cd_{0.2}S White Quantum Dots

Chin-Chuan Huang¹, Kuo-Hsiung Chu², Chin-Wei Sher^{3,*}, Chun-Liang Lin^{4,5,*}, Yan-Kuin Su^{4,5}, Chia-Wei Sun² and Hao-Chung Kuo²

- ¹ Department of Electrical Engineering, Institute of Microelectronics, National Cheng Kung University, Tainan 701401, Taiwan; q18951188@ncku.edu.tw
- ² Department of Photonics and Institute of Electro-Optical Engineering, College of Electrical and Computer Engineering, National Chiao Tung University & National Yang Ming Chiao Tung University, Hsinchu 30010, Taiwan; martinchu.eo05g@g2.nctu.edu.tw (K.-H.C.); chiawesun@faculty.nctu.edu.tw (C.-W.S.); haockuo@faculty.nctu.edu.tw (H.-C.K.)
- ³ Fok Ying Tung Institute, Hong Kong University of Science and Technology, Nansha 511458, China
- ⁴ Green Energy Technology Research Center, Kun Shan University, Tainan 71000, Taiwan; yksu@mail.ncku.edu.tw
- ⁵ Department of Electrical Engineering, Kun Shan University, Tainan 71000, Taiwan
- * Correspondence: qwshe@ust.hk (C.-W.S.); law_lin@mail.ksu.edu.tw (C.-L.L.); Tel.: +886-3-571-2121 (C.-W.S.); +886-6-205-0521 (ext. 3703) (C.-L.L.)

Abstract: In this study, we demonstrate a new design of white light-emitting diode (WLED) with high stability and luminous efficiency as well as positive aging. Colloidal ternary Zn_{0.8}Cd_{0.2}S (named Zn_{0.8}) white quantum dots (WQDs) were prepared by chemical route and dispersed in xylene, integrating them into an ultraviolet light-emitting diode (UV-LED) to form WQD-white light emitting diode (WQD-WLED). High efficiency, high color quality and excellent reliability of WQD-WLED with neutral white correlated color temperature (CCT) can be obtained. The experimental results indicate that the stability of relative luminous efficiency and color rendering index (CRI) of the WQD-WLED can reach up to 160 and 82%, respectively. Moreover, the WQD-WLED can operate more than 1000 h under 100 mA, and the quantity of WQDs in the glass package can be reduced.

Keywords: quantum dots; ultraviolet; CdSe/ZnS; luminous efficiency



Citation: Huang, C.-C.; Chu, K.-H.; Sher, C.-W.; Lin, C.-L.; Su, Y.-K.; Sun, C.-W.; Kuo, H.-C. High Stability of Liquid-Typed White Light-Emitting Diode with Zn_{0.8}Cd_{0.2}S White Quantum Dots. *Coatings* **2021**, *11*, 415. <https://doi.org/10.3390/coatings11040415>

Received: 23 February 2021

Accepted: 29 March 2021

Published: 2 April 2021

Publisher's Note: MDPI stays neutral with regard to jurisdictional claims in published maps and institutional affiliations.



Copyright: © 2021 by the authors. Licensee MDPI, Basel, Switzerland. This article is an open access article distributed under the terms and conditions of the Creative Commons Attribution (CC BY) license (<https://creativecommons.org/licenses/by/4.0/>).

1. Introduction

Recently, the phosphor-converted white light-emitting diode (WLED) has attracted a significant amount of attention due to its low material cost, good thermal stability, longer lifetime, higher luminous efficiency and environmental sustainability for solid-state lighting (SSL) [1–3]. Nowadays, the main trend for SSL application is looking towards new materials and designs to show a better light quality to match the department of energy's (DOE) demands. Therefore, to enhance the color rendering index (CRI) value and R9 is very important [4–6]. For commercial WLEDs, the blending of high efficiency red phosphors with Y₃Al₅O₁₂ (YAG) to improve CRI of WLEDs has been reported [7,8]. Moreover, to combine the different sizes of quantum dots (QDs) with an InGaN chip to obtain WLED devices with improved CRI and efficiency can be achieved [9–15]. Cyan, green, yellow and red CdSe/ZnS core/shell nanocrystals on a 452 nm blue LED with Ra of 71.07 [9]. A green and red-emitting CdSe/ZnS core-shell QDs are hybridized on a blue InGaN/GaN LED emitting at 452 nm. A high-quality white light CRI of 81 was achieved [10]. The luminous efficiency of single-phosphor (580 nm CdSe QDs) WLEDs was 5.62 lm/W_{electric} with a CRI of 15.7, whereas the luminous efficiency of dual-phosphors (555 and 625 nm CdSe QDs) WLEDs was 3.79 lm/W_{electric} with a CRI of 61.4 at 20 mA [11]. Hybridization of luminescent copolymer and yellow and red QDs forming WLEDs showed the CRI of up to 90 and their luminous efficiency was 17 lm/W_{electric} [12]. The fabricated

CdSe/CdS/ZnS core/multishell QD based-WLED exhibits a high CRI of 88 and a luminous efficiency of 32 lm/W_{electric} [15]. It has been reported that WLEDs with hybrid polymer and QDs possess excellent CRI values [13–15]. However, it was noticed that the compatibility between polymer and QDs is generally not as good, resulting in low luminous efficiency and poor stability.

Moreover, in the past, the self-absorption caused by mixing red, green and blue QDs involves a more complicated and time-consuming process for the fabrication of white light devices because it needs to control the emission wavelengths and mixing concentrations of different color QDs. The white light emission QDs (WQDs) can avoid the self-absorption problem because of two emissions covering the entire visible spectra. One is band edge emission, the other is surface-state emission. Some encapsulation materials, such as silicone, are used to protect WQDs; however, the cross link between oligomer and hardener is inhibited due to the existence of N and P elements coming from the capping reagents, hexadecylamine (HDA) and tri-n-octylphosphine oxide (TOPO) [16]. In order to overcome the poor stability and low efficiency of WQD-based WLED, the remote typed of WLED is used [17,18]. The stability and luminous efficiency of the device is also low, due to the aggregation of WQDs in the polymer matrix. In the literature, the combination of commercial UV-LED (400 nm) and a thin coating of magic-sized CdSe (quantum yield (QY) 2–3%) in polyurethane or use of high-power UV-LED to pump the white QDs (WQDs) [19,20]. Unfortunately, the luminous efficiency is quite low. Another type of WQDs, CdS with 17% of QY, is also incorporated with PMMA and dispensed on the top of a GaN based UV-LED chip [9,21,22] to form WLED. However, the luminous efficiency is also low. In our previous study, we have demonstrated that the stability and QY of Zn_{0.8} WQDs can be improved by addition of Zn element [23,24], and the luminous efficiency of Zn_{0.8} WQD-based WLED is between 4 to 12 lm/W_{electric} [16–18]. However, the luminous efficiency and stability of Zn_{0.8} WQD-based WLED is still not high enough for application in SSL.

As we know, the QY of QDs in solution is higher than that in the powder type or that which disperses in a polymer matrix. As we published before, QDs dispersed in solvent can maintain the QY for a long time [25,26]. Therefore, using liquid-type QDs is one of the strategies to improve the performance of QDs-based WLED. Most of those devices, using the special WQDs as light converting materials in liquid-type QD-based WLED is a new type of WLED to match the DOE demands in the SSL without self-absorption between different colors of monochromatic QDs, and it is important to design a container that liquid-type WQD can be well sealed inside without solvent evaporation.

In this study, the liquid-type WQDs is demonstrated as an efficient color-conversion material in WLED by pumping them with 385 nm UV-LED. We designed a glass box to protect the white light Zn_{0.8}Cd_{0.2}S (named Zn_{0.8}) QDs to keep it at a liquid state. This method can increase the luminous efficiency and reliability of WQDs-based devices. The liquid-type WQD LED (LWQD-WLED) demonstrates that the luminous efficiency, color rendering index (CRI), and correlated color temperature (CCT) of devices are 5 lm/W_{electric} higher than 80 and 4360 K, respectively. Furthermore, more than a 160% improvement after operating for 1000 h under 100 mA applied current can be obtained for the LWQD-WLED. The ultra-high stability and luminous efficiency of the device means that progress towards outstanding performance of commercially viable solid-state lighting has been made.

2. Experiment

WQD was prepared by the chemical method from the Wang, K.W. research team [27]. The emission spectrum and intensity of WQD were measured by the Horiba, FL-3 system (HORIBA, Edison, NJ, USA). Two types of devices were fabricated at the same time for comparison: one is the remote-type WQD-WLED (as our reference sample, RWQD-WLED), and the other is the liquid-type WQD WLED device (LWQD-WLED). Figure 1a shows the flowchart of the RWQD-WLED. The lead frame type UV-LED with 5.0 mm in width, 7.0 mm in length was filled with poly (dimethyl siloxane) (PDMS) and cured at 100 °C

for 1 h. The emission wavelength of UV-LED is 385 nm, the chip size is 45 mil \times 45 mil, nominal power output (EpiStar EV-D45A) is 240 mW at 350 mA and the optical power (watts)/electrical power (watt) ratio is 9.1%. Zn_{0.8} WQDs are dispersed in PMMA to form an illuminating layer and put it on the surface of the previous UV-LED. Figure 1b illustrates the flowchart of LWQD-WLED. The procedure is as follows: First, to decrease the gap between the glass, use a glass ring with 50 mm of the inner radius and 70 mm of outer radius. Then, drill a hole on the glass ring. The top and bottom substrate was cut into thin strips with the size of 3.0 cm \times 1.5 cm. Second, take the glass ring and sandwich it between two larger pieces of glass substrate. Third, leave a proper gap so that air can ventilate when QD solution is injected. Finally, seal the gaps with epoxy-based glue to finish the LWQD-WLED process. The thickness of the glass substrate is 0.1 cm and thus the overall volume, which can accommodate liquid-type WQDs, is 0.5 cm \times 0.5 cm \times π \times 0.1 cm = 0.0785 cm³. The silicone is applied on the lead frame cup by a direct dispersing method. Under normal operation, the driving current of UV-LED is 100 mA and the normal power is 43 mW. Considering the area of the lead frame type package, which is 0.25 cm², the pumping intensity is 173 mW/cm². Both RWQD-WLED and LWQD-WLED are fabricated with the same QDs and measured the performance of devices under the same conditions (e.g., the same UV chip, the same humidity, and temperature).

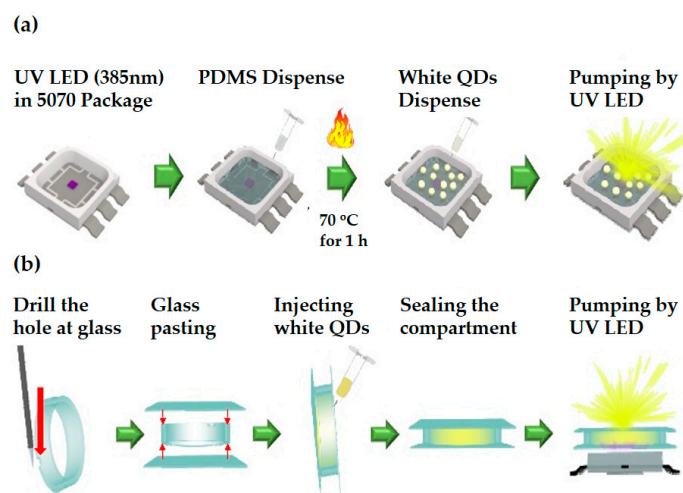


Figure 1. Schematic diagram of (a) RWQD-WLED and (b) LWQD-WLED.

3. Measurement and Analysis

Figure 2a shows the excitation and emission spectra of WQDs. The band edge and surface state emission wavelength are located at 407 and 508 nm, respectively. Based on the excitation spectrum we find that UV-LED with 385 nm is suitable for pumping WQDs. The finished liquid-type WQD glass container without and with UV light pumping is shown in Figure 2b,c, respectively.

The WQDs with different concentrations and optimization procedures were carried out to obtain similar CCTs and the best CRI values. The quantity of WQDs can determine the final color quality of the device. Microbalances (TAIWAN SCALE MFG Co, New Taipei, Taiwan) were used to precisely measure the weight of WQDs. The CCT and CRI of the reference and liquid QD samples are listed in Table 1. The bulk density of QD in RW and LW devices is not the same because we cannot measure the bulk density of QD very precisely, so it can only be used to achieve the same color temperature for comparison. In other words, the reference point for comparison is the same color temperature, rather than the bulk density of the QD. In addition, because we use the same type of light source, and the same brightness, we preset the luminous surface to be the same.

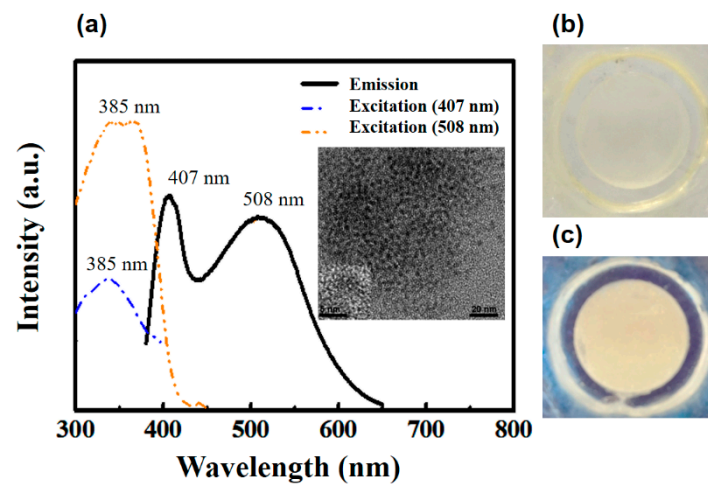


Figure 2. (a) Excitation and emission spectra of WQDs. The inset in (a) is the TEM image of WQDs. The photographs of liquid-type WQD in the glass package for (b) before UV LED pumping and (c) after UV LED pumping.

Figure 3a,b shows the electroluminescence (EL) spectra (C&M TECH. Co., Hsinchu, Taiwan) of RWQD-WLED and LWQD-WLED under the injection current from 10 mA to 100 mA. The inset in Figure 3a is the current-dependent integrated intensity of surface state emission. The current-dependent integrated intensity of the RWQD-WLED and LWQD-WLED is shown in Figure 3c. Table 1 shows the efficiency and CRI at a current of 100 mA. The values of LWQD-WLED are higher than RWQD-WLED. All measurements were performed under a calibrated integrated sphere. From the data, we find an overall improvement of 17% between liquid and remote samples at 100 mA driving current.

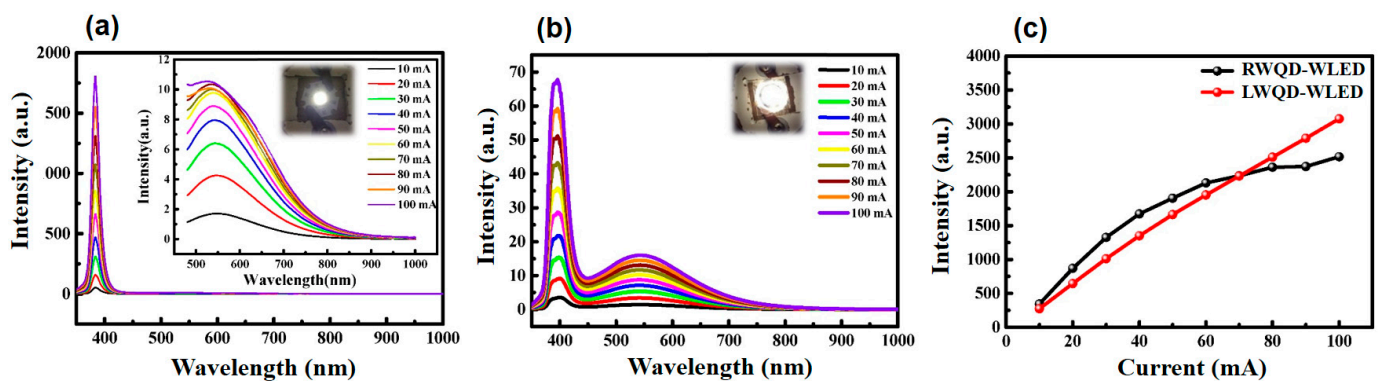


Figure 3. (a) RWQD-WLED emission spectra of the different currents and (b) LWQD-WLED emission spectra under different currents. (c) current-dependent integrated intensity of two types of devices. The insets in Figure 3a,b are the RWQD-WLED and LWQD-WLED lighting conditions.

Table 1. The efficiency and CRI of two types of devices at current of 100 mA.

Device	Operating Current	CCT (K)	CRI
RWQD-WLED	100 mA	5750	84
LWQD-WLED	100 mA	5757	80

The surface temperature of two different types of device is measured by an IR image under different applied current, and the results are shown in Figure 4a. Based on the results, we find that the surface temperature of RWQD-WLED rises with increasing applied currents, while a surface temperature lower than 30 °C even at 250 mA can be observed for LWQD-WLED. However, the surface temperature can reach 100 °C at 250 mA in the

RWQD-WLED. Figure 4b shows the thermal images of RWQD-WLED in 100 mA. On the one hand, high surface temperature will reduce the efficiency of WQDs and cause reliability problem [28]. On the other hand, the LWQD-WLED can keep the surface temperature as low as 30 °C, and the thermal images of LWQD-WLED in 100 mA is shown in Figure 4c. We know that the thermal conductivity of the glass is 1.05 W/mK, while the PMMA is 0.167–0.25 W/mK because of the poor thermal conductivity of PMMA and the heat generated from the UV-LED chip cannot be released, resulting in temperature increases with applied current, especially for high applied current. However, the liquid-type WQD solution is sealed in the glass container with much better thermal conduction and a much larger area to dissipate the heat. These facts lead to a much lower surface temperature in liquid-type devices. This has the benefit of improving the reliability of LWQD-WLED.

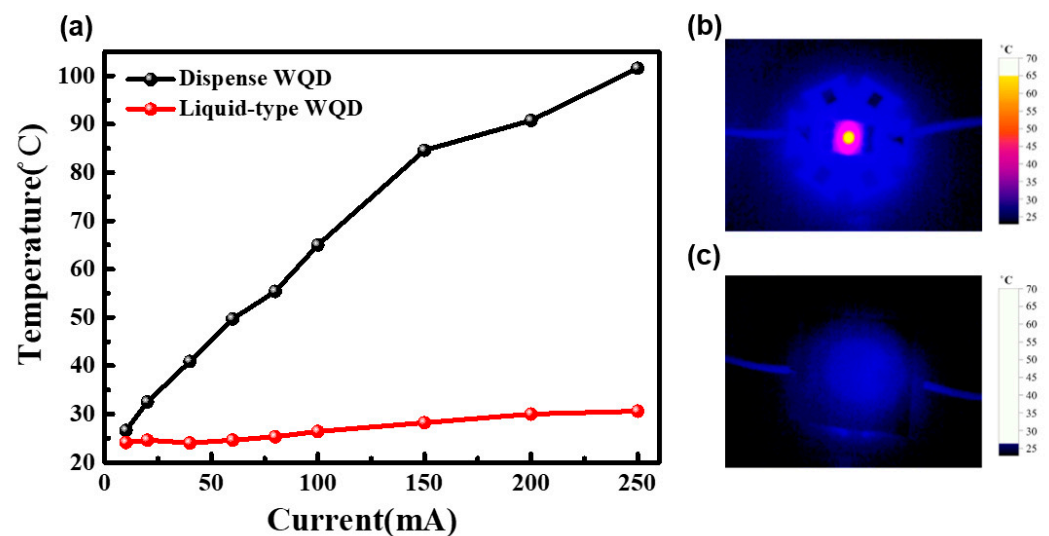


Figure 4. (a) Surface temperature of RWQD-WLED and LWQD-WLED. (b) IR images of surface temperature image of RWQD-WLED and (c) LWQD-WLED at 100 mA driving current.

Invoking Fourier's law of heat conduction, the thermal resistance (R) can be calculated as [29,30]:

$$\text{heat - transfer - rate} = \frac{\Delta T}{R}; R \propto \frac{L}{\kappa A} \quad (1)$$

where ΔT is the temperature difference between two end points and R is the thermal resistance. In this simplified model, we find the thermal conductivity and surface area of the device that affects the temperature difference significantly. From the calculation of effective emission area, the heat dissipation capacity between RWQD- and LWQD-WLED is quite different. The effective area of the LWQD-WLED device is 1.34 cm², while in RWQD-WLED it is only 0.25 cm². Therefore, much larger thermal resistance (34 times under one-dimensional analysis) in the RWQD-WLED case is expected. This is the major cause of the higher surface temperature detected. High heat trapped inside the package can certainly reduce the efficiency of WQDs, while the liquid WQD will have a larger footprint and take up more space for setup.

Figure 5a,c shows photographs of RWQD-WLED and LWQD-WLED. After driving 350 mA, photographs of RWQD-WLED and LWQD-WLED are shown in Figure 5b,d. By properly choosing the concentrations of WQDs, both devices can achieve similar CCT (5757 K) and high CRI (>80).

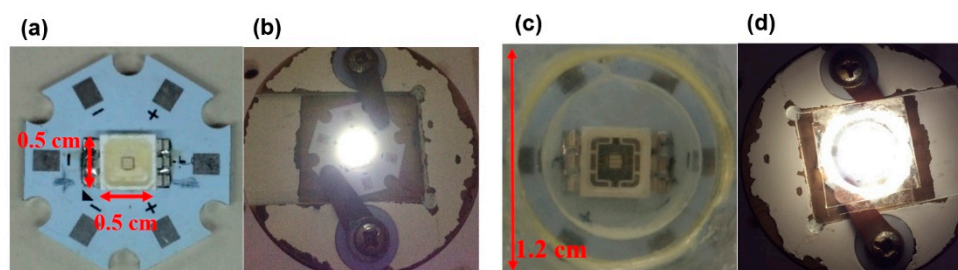


Figure 5. Photograph of (a) RWQD-WLED before UV excitation, (b) RWQD-WLED under UV-LED excitation, (c) LWQD-WLED before UV-LED excitation, (d) LWQD-WLED under UV-LED excitation.

After initial characterization of the devices, the next important task is to test the longevity of the LWQD-WLED. In the past, one result shows that serious performance degradation of the WQD-based WLED is the agglomeration of QDs and higher surface temperature when the QD disperses in polymer matrix [16–18,27,29]. In the liquid type of WQDs, the serious degradation of QY is due to the desorption of capping reagents and exposure to air [25]. When the WQD liquid is sealed in the glass compartment, it not only prevents the solvent evaporating, but it also keeps it away from oxygen and water to prevent it reacting with WQDs. We hope this can help to preserve the QY of the WQDs over a long period of time. Figure 6a,b shows the EL emission spectra of RWQD-WLED and LWQD-WLED taken at various time. The surface state emission intensity of RWQD-WLED decreases, while it increases with operation time for LWQD-WLED, indicating that the density of surface mid gap increases. The relative luminous efficiency reduction in the RWQD-WLED is 75% after a 1000 h operation, while the enhancement of about 160% for LWQD-WLED is shown in Figure 6c,d. The experimental results demonstrate that the LWQD-WLED has a stable and sustainable performance over a long period of time, as shown in Figure 6c. The CRI shifts between 0 to 1000 h for the RWQD-WLED and LWQD-WLED as shown in Figure 6d. It is found that the CRI of both devices becomes stable after 400 h. However, the CRI value goes down to 0 after 800 h for RWQD-WLED due to severe surface emission decay. From these results, it can be seen that the LWQD-WLED not only enhances its intensity but also maintains its color quality over a long period of time. This might be due to the photo annealing [31,32] and thin oxide layer [33] in liquid-type WQDs.

We observe very little change in CRI between 0 to 1000 h for LWQD-WLED. Certainly, the nature of this storage test eliminates extreme thermal and aggregation issues for the liquid WQD samples. Stable performance may demonstrate a potential solution for long-term stability in this LWQD-type device.

For WQD-based WLED, the color deviation with the different structure is used to evaluate the color stability for high-quality lighting applications. Therefore, the chromaticity coordinate shifts of RWQD-WLED and LWQD-WLED are recorded and shown in Figure 7a,b. After a long period of operation, the chromaticity coordinates for LWQD-WLED are stable. From the experimental results, RWQD-WLED shows moderate CIE coordinate-shift, while the LWQD-WLED remains at almost the same position after 1000 h of operating time. This clearly demonstrates the superiority of our design in terms of light quality which should be crucial for the next generation light source.

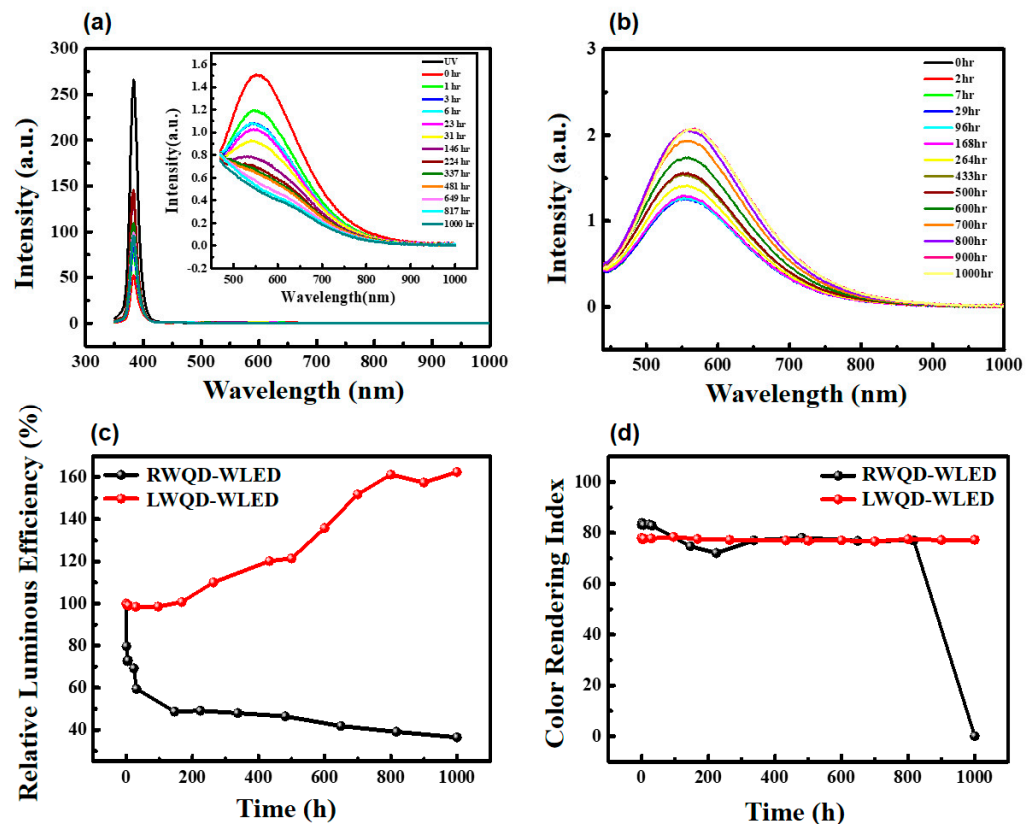


Figure 6. (a) The relative emission spectrum of the RWQD-WLED under various operation time, (b) The relative emission spectrum of the LWQD-WLED with various operation time. The lifetime character of (c) changing about relative luminous efficiency and (d) CRI between RWQD- and LWQD-WLED from 0 h to 1000 h. The inset in Figure 6. (a) is the QD part of the composition of the RWQD-WLED emission spectrum.

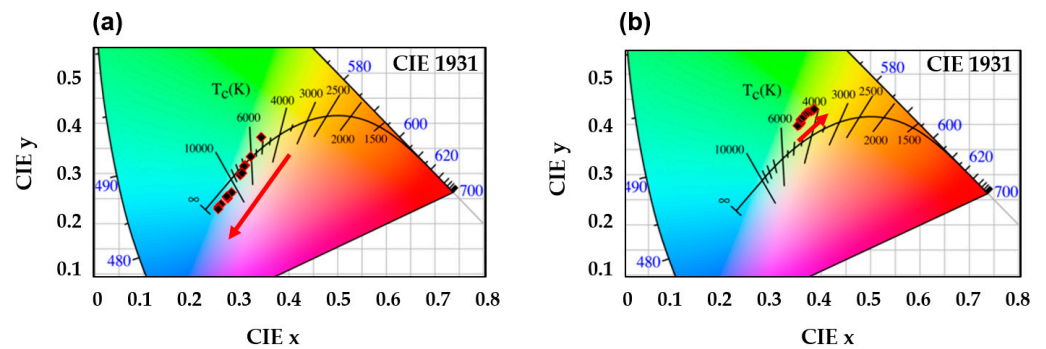


Figure 7. The chromaticity coordinate shift of WLED from 0 h to 1000 h. (a) RWQD-WLED and (b) LWQD-WLED.

4. Conclusions

This study demonstrates the direct emission white light of $Zn_{0.8}$ QDs when sealed in a glass plate in liquid type to form WLED. The LWQD-WLED shows an excellent stability and high CRI. A glass-slide is formed by the cavity and is used to protect WQDs from environmental influences. Liquid-type WQD sealed in a glass plate can maintain the CRI, keeping the original QY of WQD in solution and reducing thermal effects. This design can easily modify the emission spectra and enhance the stability of CCT and CRI of devices. LWQD-WLED were pumped by UV-LED, and showed a 160% enhancement after operating for 1000 h. The relative luminous efficiency reduction in the RWQD-WLED

is 75% after 1000 h operation, while an enhancement of about 160% for LWQD-WLED was demonstrated. The RWQD-WLED shows moderate CIE coordinate-shift, while the LWQD-WLED remains at almost the same position after 1000 h of operating time. In the future, we believe that the LWQD-WLED with high luminous efficiency and reliability is suitable for high-quality lighting applications.

Author Contributions: Conceptualization, C.-C.H., K.-H.C., and C.-W.S. (Chin-Wei Sher); Methodology, C.-C.H., K.-H.C., and C.-W.S. (Chin-Wei Sher); Validation, C.-C.H., K.-H.C., C.-W.S. (Chin-Wei Sher), C.-L.L., Y.-K.S., C.-W.S. (Chia-Wei Sun), and H.-C.K.; Formal Analysis, C.-C.H., K.-H.C., and C.-W.S. (Chin-Wei Sher); Resources, C.-C.H., K.-H.C., C.-W.S. (Chin-Wei Sher), C.-L.L., Y.-K.S., C.-W.S. (Chia-Wei Sun), and H.-C.K.; Data Curation, C.-C.H., K.-H.C., C.-W.S. (Chin-Wei Sher), C.-L.L., Y.-K.S., C.-W.S. (Chia-Wei Sun) and H.-C.K.; Writing—Original Draft Preparation, C.-C.H., K.-H.C. and C.-W.S. (Chin-Wei Sher); Writing—Review and Editing, C.-C.H., K.-H.C., C.-W.S. (Chin-Wei Sher), C.-L.L., Y.-K.S., C.-W.S. (Chia-Wei Sun), and H.-C.K. All authors have read and agreed to the published version of the manuscript.

Funding: This work was supported in part by the Ministry of Science and Technology of Taiwan, under Grant MOST 107-2221-E006-185-MY3 and Grant 108-2221-E-006-201-MY3, and in part by the Green Energy Technology Research Center, Department of Electrical Engineering, Kun Shan University, Tainan, Taiwan through The Featured Areas Research Center Program within the framework of the Higher Education Sprout Project by the Ministry of Education (MOE) in Taiwan.

Institutional Review Board Statement: Not applicable.

Informed Consent Statement: Not applicable.

Data Availability Statement: Not applicable.

Acknowledgments: The authors gratefully acknowledge the support from the Institute of Microelectronics, National Cheng Kung University and Green Energy Technology Research Center, Kun Shan University, Taiwan. The author is particularly grateful to Dr. Sher of the Hong Kong University of Science and Technology.

Conflicts of Interest: The authors declare no conflict of interest.

References

1. Chen, K.J.; Chen, H.C.; Tsai, K.A.; Lin, C.C.; Tsai, H.H.; Chien, S.H.; Cheng, B.S.; Hsu, Y.J.; Shih, M.H.; Tsai, C.H.; et al. Resonant-enhanced full-color emission of quantum-dot-based display technology using a pulsed spray method. *Adv. Func. Mater.* **2012**, *22*, 5138–5143. [[CrossRef](#)]
2. Gu, P.; Zhang, Y.; Feng, Y.; Zhang, T.; Chu, H.; Cui, T.; Wang, Y.; Zhao, J.; Yu, W.W. Real-time and on-chip surface temperature sensing of GaN LED chips using PbSe quantum dots. *Nanoscale* **2013**, *5*, 10481–10486. [[CrossRef](#)] [[PubMed](#)]
3. Jang, H.S.; Yang, H.; Kim, S.W.; Han, J.Y.; Lee, S.G.; Jeon, D.Y. White light-emitting diodes with excellent color rendering based on organically capped CdSe quantum dots and Sr₃SiO₅:Ce³⁺,Li⁺ Phosphors. *Adv. Mater.* **2008**, *20*, 2696–2702. [[CrossRef](#)] [[PubMed](#)]
4. Lee, J.; Sundar, V.C.; Heine, J.R.; Bawendi, M.G.; Jensen, K.F. Full color emission from II–VI semiconductor quantum dot–polymer composites. *Adv. Mater.* **2000**, *12*, 1102–1105. [[CrossRef](#)]
5. Clapp, A.R.; Medintz, I.L.; Uyeda, H.T.; Fisher, B.R.; Goldman, E.R.; Bawendi, M.G.; Mattoussi, H. Quantum dot-based multiplexed fluorescence resonance energy transfer. *J. Am. Chem. Soc.* **2005**, *127*, 18212–18221. [[CrossRef](#)]
6. Reiss, P.; Bleuse, J.; Pron, A. Highly luminescent CdSe/ZnSe core/shell nanocrystals of low size dispersion. *Nano Lett.* **2002**, *2*, 781–784. [[CrossRef](#)]
7. Shirasaki, Y.; Supran, G.J.; Bawendi, M.G.; Bulovic, V. Emergence of colloidal quantum-dot light-emitting technologies. *Nat. Photon.* **2013**, *7*, 13–23. [[CrossRef](#)]
8. Jang, E.; Jun, S.; Jang, H.; Lim, J.; Kim, B.; Kim, Y. White-light-emitting diodes with quantum dot color converters for display backlights. *Adv. Mater.* **2010**, *22*, 3076–3080. [[CrossRef](#)]
9. Nizamoglu, S.; Ozel, T.; Sari, E.; Demir, H.V. White light generation using CdSe/ZnS core-shell nanocrystals hybridized with InGaN/GaN light emitting diodes. *Nanotechnology* **2007**, *18*, 065709. [[CrossRef](#)]
10. Nizamoglu, S.; Zengin, G.; Demir, H.V. Color-converting combinations of nanocrystal emitters for warm-white light generation with high color rendering index. *Appl. Phys. Lett.* **2008**, *92*, 031102. [[CrossRef](#)]
11. Chung, W.; Park, K.; Yu, H.J.; Kim, J.; Chun, B.H.; Kim, S.H. White emission using mixtures of CdSe quantum dots and PMMA as a phosphor. *Opt. Mater.* **2010**, *32*, 515–521. [[CrossRef](#)]

12. Lin, H.Y.; Wang, S.W.; Lin, C.C.; Chen, K.J.; Han, H.V.; Tu, Z.Y.; Tu, H.H.; Chen, T.M.; Shih, M.H.; Lee, P.T.; et al. Excellent color quality of white-light-emitting diodes by embedding quantum dots in polymers material. *IEEE J. Sel. Top. Quan. Elect.* **2016**, *22*, 35–41. [[CrossRef](#)]
13. Nizamoglu, S.; Erdem, T.; Sun, X.W.; Demir, H.V. Warm-white light-emitting diodes integrated with colloidal quantum dots for high luminous efficacy and color rendering. *Opt. Lett.* **2010**, *35*, 3372–3374. [[CrossRef](#)]
14. Nizamoglu, S.; Mutlugun, E.; Özel, T.; Demir, H.V.; Sapra, S.; Gaponik, N.; Eychemüller, A. Dual-color emitting quantum-dot-quantum-well CdSe-ZnS heteronanocrystals hybridized on InGaN/GaN light emitting diodes for high-quality white light generation. *Appl. Phys. Lett.* **2008**, *92*, 113110. [[CrossRef](#)]
15. Wang, X.; Li, W.; Sun, K. Stable efficient CdSe/CdS/ZnS core/multi-shell nanophosphors fabricated through a phosphine-free route for white light-emitting-diodes with high color rendering properties. *J. Mater. Chem.* **2011**, *21*, 8558–8565. [[CrossRef](#)]
16. Siao, C.B.; Wang, K.W.; Chen, H.S.; Su, Y.S.; Chung, S.R. Ultra high luminous efficacy of white $Zn_xCd_{1-x}S$ quantum dots-based white light emitting diodes. *Opt. Mater. Express* **2016**, *6*, 749–758. [[CrossRef](#)]
17. Hsu, S.C.; Chen, Y.H.; Tu, Z.Y.; Han, H.V.; Lin, S.L.; Chen, T.M.; Kuo, H.C.; Lin, C.C. Highly stable and efficient hybrid quantum dot light-emitting diodes. *IEEE Photonics J.* **2015**, *7*, 1–10. [[CrossRef](#)]
18. Chen, Y.C.; Siao, C.B.; Chen, H.S.; Wang, K.W.; Chung, S.R. The application of $Zn_{0.8}Cd_{0.2}S$ nanocrystals in white light emitting diodes devices. *RSC Adv.* **2015**, *5*, 87667–87671. [[CrossRef](#)]
19. Bowers, M.J.; McBride, J.R.; Rosenthal, S.J. White-light emission from magic-sized cadmium selenide nanocrystals. *J. Am. Chem. Soc.* **2005**, *127*, 15378–15379. [[CrossRef](#)]
20. Schreuder, M.A.; Gosnell, J.D.; Smith, N.J.; Warnement, M.R.; Weiss, S.M.; Rosenthal, S.J. Encapsulated white-light CdSe nanocrystals as nanophosphors for solid-state lighting. *J. Mater. Chem.* **2008**, *18*, 970–975. [[CrossRef](#)]
21. Kshirsagar, A.; Pickering, S.; Xu, J.; Ruzyllo, J. Light emitting diodes formed using mist deposition of colloidal solution of CdSe nanocrystalline quantum dots. *ECS Trans.* **2011**, *35*, 71–77. [[CrossRef](#)]
22. Huang, H.T.; Tsai, C.C.; Huang, Y.P. Conformal phosphor coating using pulsed spray to reduce color deviation of white LEDs. *Opt. Express* **2010**, *18*, A201–A206. [[CrossRef](#)]
23. Chen, Y.C.; Chen, H.S.; Chung, S.R.; Chang, J.K.; Wang, K.W. The effect of surface structures and compositions on the quantum yields of highly effective $Zn_{0.8}Cd_{0.2}S$ nanocrystals. *J. Mater. Chem. C* **2015**, *3*, 5881–5884. [[CrossRef](#)]
24. Chen, H.S.; Chung, S.R.; Chen, Y.C.; Chen, T.Y.; Liu, C.Y.; Wang, K.W. The structure-dependent quantum yield of ZnCdS nanocrystals. *Cryst. Eng. Comm.* **2015**, *17*, 5032–5037. [[CrossRef](#)]
25. Sher, C.W.; Lin, C.H.; Lin, H.Y.; Lin, C.C.; Huang, C.H.; Chen, K.J.; Li, J.R.; Wang, K.Y.; Tu, H.H.; Fu, C.C.; et al. A high quality liquid-type quantum dot white light-emitting diode. *Nanoscale* **2016**, *8*, 1117–1122. [[CrossRef](#)] [[PubMed](#)]
26. Chen, H.S.; Chung, S.R.; Chen, T.Y.; Wang, K.W. Graphene-supported Pt and PtPd nanorods with enhanced electrocatalytic performance for the oxygen reduction reaction. *J. Mater. Chem. C* **2014**, *2*, 2664–2667. [[CrossRef](#)]
27. Chen, H.S.; Wang, K.W.; Chen, S.S.; Chung, S.R. $Zn_xCd_{1-x}S$ quantum dots-based white light-emitting diodes. *Opt. Lett.* **2013**, *38*, 2080–2082. [[CrossRef](#)] [[PubMed](#)]
28. Chen, K.J.; Chen, H.C.; Shih, M.H.; Wang, C.H.; Kuo, M.Y.; Yang, Y.C.; Lin, C.C.; Kuo, H.C. The influence of the thermal effect on CdSe/ZnS quantum dots in light-emitting diodes. *J. Lightwave Technol.* **2012**, *30*, 2256–2261. [[CrossRef](#)]
29. Erdem, T.; Nizamoglu, S.; Demir, H.V. Computational study of power conversion and luminous efficiency performance for semiconductor quantum dot nanophosphors on light-emitting diodes. *Opt. Express* **2012**, *20*, 3275–3295. [[CrossRef](#)]
30. Incropera, F.P.; DeWitt, D.P.; Bergman, T.L.; Lavine, A.S. *Fundamentals of Heat and Mass Transfer*, 6th ed.; John Wiley & Sons, Inc.: Hoboken, NJ, USA, 2005; Volume 4, pp. 58–66.
31. Kim, K.; Woo, J.Y.; Jeong, S.; Han, C.S. Photoenhancement of a quantum dot nanocomposite via UV annealing and its application to white LEDs. *Adv. Mater.* **2011**, *23*, 911–914. [[CrossRef](#)]
32. Kimura, J.; Uematsu, T.; Maenosono, S.; Yamaguchi, Y. Photoinduced fluorescence enhancement in CdSe/ZnS quantum dot submonolayers sandwiched between insulating layers: Influence of dot proximity. *J. Phys. Chem. B* **2004**, *108*, 13258–13264. [[CrossRef](#)]
33. Zhang, T.; Zhao, H.; Riabinina, D.; Chaker, M.; Ma, D. Concentration-dependent photoinduced photoluminescence enhancement in colloidal PbS quantum dot solution. *J. Phys. Chem. C* **2010**, *114*, 10153–10159. [[CrossRef](#)]